Preparation and Characterization of Activated Palm Kernel Shell/Carboxylated Nitrile Butadiene Rubber (APKS/XNBR) Vulcanizate

Syazwani Aqilah Zainal[1], Siti Nur Liyana Mamauod [1,2], Nahrul Hayawin Zainal[3], Hanafi Ismail[4], Muhammad Ilham Mamauod[5]*

[1]Faculty of Applied Sciences, Universiti Teknologi MARA (UiTM), 40450 Shah Alam, Selangor, MALAYSIA
[2]Centre of Chemical Synthesis and Polymer Technology (CCSPT), Institute of Science, Universiti Teknologi MARA, 40450 Shah Alam, Selangor, MALAYSIA
[3]Green Products Development, Biomass Technology Unit, Engineering and Processing Division, Malaysian Palm Oil Board, MALAYSIA
[4]School of Materials & Mineral Resources Eng., USM Eng. Campus, 14300 Nibong Tebal, Penang, MALAYSIA
[5]Industrial Chemical Technology, Faculty of Science & Technology, Universiti Sains Islam Malaysia (USIM), Bandar Baru Nilai71800, Nilai, Negeri Sembilan, MALAYSIA
[*]nurliyana2219@uitm.edu.my

ABSTRACT

Malaysia is one of the most important palm oil producers and exporters in the whole wide world. There has been a rapid development of new palm oil plantations and palm oil mills in this country. The palm oil industry plays a vital role in the economic growth of Malaysia. However, as the palm oil industry grows bigger and wider, a huge amount of palm oil waste is produced which is an alarming issue considering it can cause pollution and have a negative effect on the environment. Raw Palm Kernel Shell (PKS) derived from palm oil waste can be converted into Activated Palm Kernel Shell (APKS) which has the potential to be a value-added biofiller in rubber vulcanizates. Thus, in this study, APKS is prepared through a carbonization process at a temperature of 900 °C and an activation process via steam treatment and used as filler in Carboxylated Nitrile Butadiene Rubber (XNBR). The aim of this study is to evaluate the influence of different loading ratios of APKS on the

ISSN 1823-5514, eISSN 2550-164X
Received for review: 2022-11-17
Accepted for publication: 2023-10-30
Published: 2024-01-15

https://doi.org/10.24191/jmeche.v21i1.25368

swelling index measurement, bound rubber content (BRC), abrasion resistance, compression set, and hardness of XNBR vulcanizates. APKS is incorporated in XNBR at different loading ratios, ranging from 0 to 50 phr and these APKS-filled XNBR vulcanizates are prepared with a two-roll mill. The overall physico-mechanical properties of APKS-filled XNBR vulcanizates showed increment in terms of BRC, compression set, and hardness as the loading ratio of APKS increased. XNBR vulcanizates with a higher loading ratio of APKS also showed a decrease in swelling index measurement and volume loss which would indicate high abrasion resistance. These results could be attributed to the porosity of APKS as shown in the morphological analysis which provided a high surface area of contact for crosslinking and mechanical interlocking. This proves APKS could potentially be a semi-reinforcing filler for rubber vulcanizates, especially for XNBR vulcanizates as XNBR vulcanizates were able to achieve high abrasion resistance and high hardness with the incorporation of APKS. With this, the conversion of PKS into APKS could help to reduce palm oil waste and provide an environmentally friendly, sustainable biofiller option to rubber researchers and manufacturers who are looking for an alternative to petroleum-based fillers. This would be very beneficial for both the palm oil industry and the rubber industry.

Keywords: *Activated Palm Kernel Shell (APKS); Carboxylated Nitrile Butadiene Rubber (XNBR); Biofiller; Swelling Index Measurement; Physico-Mechanical Properties*

Introduction

The development of sustainable additives from biomass plays an important role in the future of mankind because of the increasing rate of greenhouse emissions, depletion of fossil fuel, and the pollutants that are hazardous to human beings [1]. The production of biomass from palm oil has increased from 15 million tons in 1995 to 66 million tons in 2017 [2]. Palm biomass which includes Palm Kernel Shell (PKS), empty fruit bunches, and mesocarp fibres is under-utilized and unsystematically disposed via open burning, leading to air pollution [3]. Direct burning of biomass produces dust emission and smoke due to incomplete combustion which is not environment friendly [4].

Recently, many efforts have been attempted to use and incorporate PKS as biofiller in rubber compounding to minimize environmental issues. This development of renewable biofiller in the rubber industry provides a novel alternative solution to improve the management of agricultural waste. Reinforcement plays an important role in rubber compounding in order to produce good performance of rubber-based products which is influenced by the surface area, size, loading, surface activity, and dispersion state of filler particles. Good interfacial interaction between rubber and filler phases

promotes the capability stress transferred from rubber chains to the filler which leads to the enhancement of physical and mechanical properties of vulcanized rubber [5]-[6].

A study of raw PKS characterization by Daud et al. [7] revealed that the surface of raw PKS is smooth which provided a small surface area, hence weaker rubber-filler interaction. In order to provide reinforcement to rubber vulcanizates, the rubber chain must make intimate contact with filler particles. Filler with a low surface area can only provide a limited contact area for crosslinking, mechanical interlocking, and rubber-filler interaction which will minimize the potential to reinforce the rubber composite. The presence of dirt, impurities, crevices, voids, and extensive filler detachment on the raw PKS surface will result in poor rubber-filler interaction. Not to mention, low reinforcement provided by the Activated Palm Kernel Shell (APKS) due to the impurities, causing high mechanical stress points and poor mechanical properties of the rubber vulcanizates. Moreover, raw PKS has low carbon content. The utilization of filler with low carbon content in rubber results in poor mechanical properties of rubber vulcanizates. A high carbon content of filler is preferable since the presence of high carbon in filler has the ability to form a strong interaction with the hydrocarbon chain in rubber [7]. The study of utilization of raw PKS in natural rubber was studied by Daud et al. [7] revealed the interaction between raw PKS and natural rubber is poor due to the presence of lignin, hemicellulose, and cellulose with 44.0%, 21.6%, and 27.7%, respectively which reduce the reinforcement in the rubber vulcanizate [8]. This raw PKS contains various polar functional groups such as ether and methoxyl, phenolic hydroxyls, carbonyl, carboxyl, aliphatic, and phenolic hydroxyls that contribute to the polarity. The high polarity of filler in rubber will contribute to the rubber-filler interaction due to the strong interaction between fillers. Strong inter- and intra-molecular interactions could cause agglomeration to occur [6]. The agglomeration of filler in rubber vulcanizate will initiate the fracture when subjected to mechanical force due to un-uniform stress distribution [9]. These weaknesses of raw PKS lead to poor reinforcement that lowers the mechanical properties of rubber vulcanizate [7].

Many studies have attempted to overcome the limitation of raw PKS. Since it has been known that raw PKS has its disadvantages, these raw PKS undergo surface treatment to enhance and improve its properties in terms of carbon content, porosity, and surface activity. These raw PKS undergo a dual process which are carbonization process and steam treatment, converting them into APKS. The steam treatment creates more pores and enlarges the existing pores that were originally produced during carbonization process. This will indirectly help to enlarge the surface area of APKS, contributing to better reinforcement. The carbonization process increases the carbon content in carbonized carbon from 46.93 wt.% to 84.77 wt.% and reduces hydrogen and oxygen content due to the dehydration process. The carbon content in filler is crucial as carbon promotes chemical interaction between rubber and filler [10].

The lignin, cellulose, and hemicellulose elements which contributed to the presence of polar functional groups in APKS will extremely decrease after the carbonization process due to dehydration and deoxygenation reaction. The degradation of polar functional groups of APKS reduced the interaction between APKS particles which can prevent the agglomeration in rubber matrix [6]. The impurities and dirt present in PKS which disturb the adsorption of rubber on the filler surface also degrade during the carbonization process. This degradation will improve the rubber-filler interaction that enhances the reinforcement of the rubber vulcanizate [11].

In this study, APKS is characterized through Fourier-Transform Infrared Spectroscopy (FTIR), Scanning Electron Microscopy (SEM)/Energy Dispersive X-ray (EDX), and Brunauer-Emmett-Teller (BET) analysis. APKS is then incorporated in Carboxylated Nitrile Butadiene Rubber (XNBR) at different loading ratios ranging from 0 to 50 phr. The performance of APKS-filled XNBR vulcanizates is evaluated by conducting some tests such as swelling measurement, BRC, abrasion resistance, compression set, and hardness. This way, the effectiveness of APKS as a potential biofiller can be proven to improve the mechanical properties of XNBR vulcanizate and utilized as a solution to reduce palm oil waste.

Experimental

Materials

APKS was purchased from the Research Institute of Malaysian Palm Oil Board (MPOB) Bangi, Malaysia while the XNBR was supplied by Aras Bakti Ventures Sdn. Bhd. Compounding ingredients, for instance, benzothiazyl disulfide (MBTS), polymerized 2, 2.4-trimethyl-1.2-dihydroquinoline (TMQ), n,n-diphenylguandine (DPG), and Tetramethylthiuram Disulfide (TMTD) were provided by Airelastic Industries Sdn. Bhd. The rest of the compounding ingredients such as zinc oxide, sulphur, stearic acid, and paraffin oil were supplied by the Faculty of Applied Science, Universiti Teknologi MARA.

Preparation of fine particles APKS

APKS purchased from MPOB were in big particle size. In order to obtain APKS with fine particle size, these APKS had to be crushed and pulverized with a crusher and pulverizer, respectively. There were then sieved through a sieve with 240 mesh size, by using a vibratory sieve shaker (Retsch AS 200, Germany).

Characterization of APKS

Fourier Transform Infrared (FTIR) analysis

FTIR is an analytical technique using infrared light to identify chemical functional groups in APKS. This analysis is important as the chemical

functional group of APKS influences its surface activity and polarity. This procedure followed ASTM E168, with the spectrum obtained using Perkin-Elmer Spectrum One Series. The spectrum resolution was 4 cm^{-1}, and the scanning range was 650 to 4000 cm^{-1}.

Scanning Electron Microscopy (SEM) and Energy Dispersive X-Ray (EDX) analysis

The surface morphology of APKS was investigated through SEM/EDX analysis. This test was conducted to identify the surface, shape, pore size, and range of particle size of a primary particle of APKS. The surface structure of APKS was observed by using a scanning electron microscope (SEM) (spectroscopy electron microscope Shimadzu SSX-550) and conducted according to ASTM F1372. The APKS samples were coated with 20-30 nm thickness of gold using a sputter coater to prevent surface charge and promote the emission of the secondary electron to provide a homogeneous surface for imaging and analysis. EDX analysis was conducted after SEM analysis to identify the presence of the element in the APKS samples.

Brunauer-Emmett-Teller (BET) analysis

BET analysis aims to determine the specific surface area and the porosity of APKS per gram. This test was conducted based on ASTM D5604. The outgassing process was carried out before analysing the surface properties of the sample. It is important to ensure that the sample has no moisture content before the outgassing process is carried out. The outgassing process took 5 to 6 hours. Helium gas was injected into the sample holder to measure the volume which was not occupied by the sample. Nitrogen was injected by successive steps after the helium evacuation, enabling the apparatus to measure the pressure in the sample holder. Then, the sample was placed in a chamber for surface area, pore volume, and pore radius analysis.

Preparation of APKS-filled XNBR vulcanizates

The formulation for APKS-filled XNBR vulcanizates is shown in Table 1. APKS of different loading ratios were mixed with XNBR by using a two-roll mill (2 OSAKA 18), according to American Standard of Testing and Material (ASTM) designation D3184-80. XNBR was first masticated to reduce the viscosity and soften the rubber. The sequence of mixing ingredients is shown in Figure 1. The APKS-filled XNBR compound was compressed by using hot compression moulding machine at a temperature of 160 °C. The compounded rubber was compressed for an amount of time, according to the cure time obtained from the cure characteristics test. The APKS-filled XNBR vulcanizates were then tested for swelling index measurement, BRC, abrasion resistance, compression set, and hardness.

Table 1: Formulation of APKS-filled XNBR vulcanizates

Ingredients	Formulation number						
	1	2	3	4	5	6	7
XNBR	100	100	100	100	100	100	100
APKS	0	5	10	20	30	40	50
Activator	5	5	5	5	5	5	5
Antioxidant	0.8	0.8	0.8	0.8	0.8	0.8	0.8
Accelerator	3.7	3.7	3.7	3.7	3.7	3.7	3.7
Sulphur	1.3	1.3	1.3	1.3	1.3	1.3	1.3
Processing oil	5	5	5	5	5	5	5

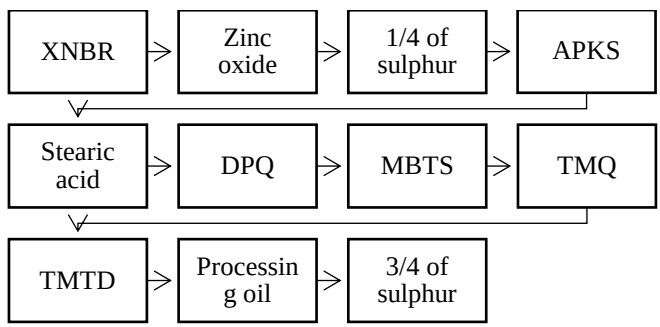

Figure 1: The mixing sequence of compounding ingredients for APKS-filled XNBR vulcanizates

Characterization of APKS-filled XNBR vulcanizates

Swelling index measurement

Swelling measurement was conducted based on ASTM D6814 and the volume fraction of rubber in the swollen gel (V_r) and swelling index were calculated according to Equations (1) and (2), respectively.

$$Vr = \frac{VR}{VR+V\prime} \qquad VR = \frac{Wo}{\rho r\prime} \qquad Vs = \frac{WSD}{\rho s} \tag{1}$$

$$Q = \frac{Wf-Wo}{Wo}\ x\ 100 \tag{2}$$

where W_o is the initial weight, $\rho r'$ *i*s the density of rubber, W_{SD} is the dissolved rubber in solvent, ρ_s is the density of solvent and W_f is the swollen weight of rubber.

BRC Analysis

BRC analysis was carried out according to ASTM D5775. Approximately, 0.25 - 0.3 g uncured rubber compound was prepared. Then the sample was

placed in a beaker that contained 50 ml of toluene. The beaker was sealed and placed in a dark place for 7 days at room temperature. After 7 days, the sample was weighed and dried for 1 - 2 hours at room temperature to allow the solvent to evaporate. Lastly, the sample was dried in a drying cabinet at a temperature of 50 °C. BRC was calculated based on Equation (3).

$$BRC\ (\%) = \frac{Wdry - Winsol}{Wo\ x \frac{Wfiller\ phr}{Wtotal\ phr}}\ x\ 100 \quad (3)$$

where *BRC* is the percent of bound rubber content, W_{dry} is the dry weight of the sample, W_{insol} is the total insoluble component of the sample in phr, W_o is the initial weight of the sample, $W_{filler.phr}$ is the phr of filler in the sample and $W_{total.phr}$ is the total phr of the sample.

Abrasion resistance

Abrasion resistance is an important property required by a rubber-based product. This test is to measure the volume loss (*VL*) of APKS-filled XNBR vulcanizates which would indicate the resistance of the vulcanizates towards the abrasive force. This test was carried out in accordance with ASTM D5963-04 by using a DIN Abrasion Resistance Tester. The *VL* was calculated based on Equation (4).

$$Volume\ loss = \ (weight\ loss)/density \quad (4)$$

Compression set

The compression set determines the ability of APKS-filled XNBR vulcanizates to maintain their elastic properties after prolonged compressive stress. The sample was prepared with a dimension of approximately 6.0 ± 0.2 mm of thickness and 3.0 ± 0.2 mm of diameter. The sample was placed between the spacers of the compression device. The sample was compressed to about 25% of its original thickness for 2 hours. After that, the sample was removed from the compression device. The thickness of the sample was measured after 30 minutes. The compression set was calculated using Equation (5) and it is expressed as the percentage of the original deflection.

$$Compression\ set = \frac{to - ti}{to - tn}\ x\ 100 \quad (5)$$

where t_o is the original thickness of the specimen, t_i is the final thickness of the specimen, and t_n is the thickness of the space bars used.

Hardness

Hardness is vital for a rubber-based product as it is the resistance from having a permanent deformation. This test was performed according to ASTM 2240 by using SUNDOO LX-A. This test was conducted to determine the relative

hardness of APKS-filled XNBR vulcanizates. The indenter used was Type A. The sample was prepared with a thickness of about 6.4 mm. Then the sample was placed on the hard and flat surface of the machine. The sample must be placed parallel to the surface of the equipment. The indenter instrument would then press into the sample until a constant hardness value is obtained.

Results and Discussion

Characterization of APKS

FTIR analysis identifies the functional groups present in APKS that contribute to the polarity and surface activity which would affect the interaction with XNBR. Figure 2 displays the FTIR spectrum obtained for the APKS sample. The broad peak obtained at the wavelength of 3749.6 cm^{-1} could be due to the presence of hydroxyl group (O-H) which was a result of the absorption of moisture on the surface of APKS [12]. The peak at 3000.3 cm^{-1} represented the C-H alkene stretching vibration from cellulose and hemicellulose degradation. This clearly indicated the presence of a lignocellulosic structure of the APKS. The peaks at bands of 2322.9 cm^{-1} and 2163.2 cm^{-1} could be attributed to the occurrence of silane (S-H) and double-bonded C-O groups, respectively. Meanwhile, the peak at 1510.8 cm^{-1} implied the C=C stretching in the aromatic ring of decomposed lignin. The peak at 1068.0 cm^{-1} indicated the presence of C-O stretching of alcohol and phenol. Both the O-H and C-O functional groups were induced from the steam treatment during the physical activation [13]. These oxygen functional groups act as an active site that contributes to the polarity of APKS [14] and enhances rubber-filler interaction with cyano (-CN) groups in XNBR thus, leading to a better distribution of APKS particles throughout the XNBR matrix [15]. A peak at 957.3 cm^{-1} indicates the C-H out-of-plane bending [11]. Similar results were reported by Ahmad et al. [16] and Ezzuldin et al. [12], in which hydroxyl (OH) groups stretching and C=C stretching vibration of an aromatic ring at a wavelength of 3347 cm^{-1} and 1575 cm^{-1}, respectively.

The surface morphology of APKS was observed by using SEM. Figure 3(a) shows the presence of a porous structure on the surface of APKS which was developed from the carbonization process. This was where the discharge of volatile matters occurred. In general, the discharge of volatile matters was due to the breakdown of the hydroxyl group in APKS, which releases H and O elements [17]. During the steam treatment, the leftover volatile matter was removed and indirectly increased the porosity of APKS enlarging the existing pores on the surface of APKS. This steam treatment process also helped to open up and remove any impurities that clogged the pores of APKS [18]. The existence of white spots on the APKS surface as labelled in Figure 3(a) could be due to the presence of ash in APKS, which the ash content of APKS was

approximately 0.82 ± 0.012%. However, the low content of ash did not affect the properties of vulcanizate [19].

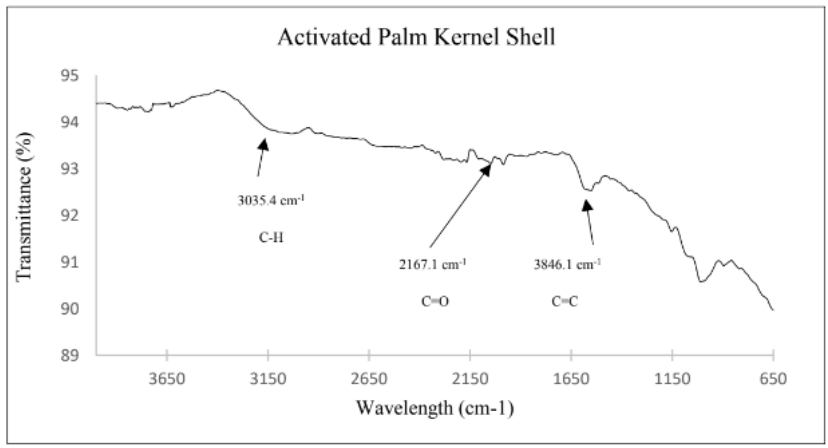

Figure 2: FTIR spectrum of APKS

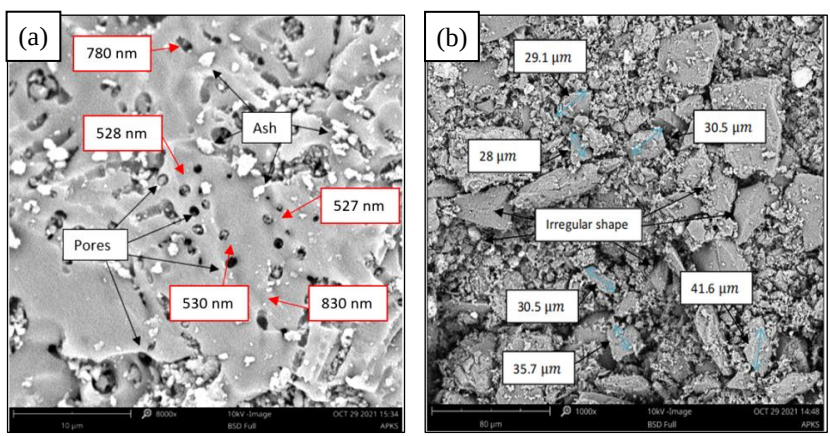

Figure 3: SEM images of; (a) APKS pores, and (b) APKS shape, and particle size at 3000x magnification

Figure 3(a) also displays the pore diameter of APKS, which ranged from 527 to 830 nm. These pores are categorized as macropores since they are larger than 50 nm [20]. With the pore diameter ranging from 527 to 830 nm, these well-developed pores helped to provide a large surface area of contact for rubber-filler interaction to take place, which would contribute to high mechanical properties [21]. As for Figure 3(b), it shows the particle size of

APKS ranged from 28.0 to 41.6 µm and that the surface of APKS looked rough with an irregular shape. The surface roughness and irregularity in the shape of APKS was attributed to APKS had undergone both carbonization and steam treatment process [22].

In order to determine the elemental composition present on the surface of APKS, APKS was analysed by using EDX analysis. Figure 4 displays the EDX spectrum of APKS. As can be seen in Figure 4, it shows the presence of different elements in APKS, including carbon (C) and oxygen (O). Based on Figure 4, APKS contained about 84.12 wt.% of carbon which could be generated from the degradation of lignin, cellulose, and hemicellulose in PKS during the carbonization process. The spectra exhibited the presence of oxygen on the APKS surface where 15.88% of oxygen composition was recorded. The presence of oxygen on the surface of APKS could be attributed to the activation process of steam treatment [13]. The oxygen content contributes to the APKS polarity and enhances the surface activity [11]. The results obtained from this EDX analysis are in accordance with the FTIR results which are shown in Figure 2.

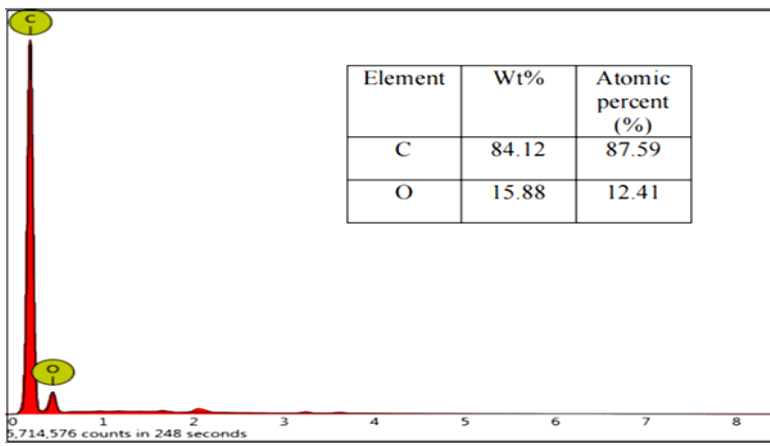

Element	Wt%	Atomic percent (%)
C	84.12	87.59
O	15.88	12.41

Figure 4: EDX spectrum of APKS

Table 2 presents the porous characteristics of APKS. This analysis is vital to investigate the contact area of APKS that is exposed to the rubber matrix. Based on the results, APKS was found to display a high BET surface area of 491.7 m^2/g. The release of volatile matter from PKS biochar during carbonization process contributed to the formation of pores in the remaining non-volatile fraction within the PKS biochar, which was then transformed into APKS [23]. The pore volume and pore radius of the APKS recorded a value of 2.323 ± 0.197 m^3/g and 513.9 ± 330.1 nm, respectively. These BET results further corroborate the surface morphology that was illustrated in Figure 3.

Table 2: Porous characteristics of APKS

Surface area	Pore volume (m^3/g)	Pore radius (nm)
491.7	2.323 ± 0.197	513.9 ± 330.1

Characterization of APKS-filled XNBR vulcanizates

The degree of swelling also known as swelling index [7] was calculated to study the ability of rubber vulcanized to resist the solvent from penetrating the crosslink network of rubber chains. The swelling index reduced as higher loading of APKS was incorporated in the XNBR vulcanizates due to better rubber-filler interaction which is indicated by the volume fraction of rubber in the swollen gel, *Vr* [24]. The volume fraction of rubber in the swollen gel, *Vr* showed an increasing trend which can be seen in Figure 5. Unfilled XNBR recorded a swelling index value of 160.72% which was the highest swelling index value among the other APKS filled XNBR vulcanizates. This showed that the unfilled XNBR vulcanizate had poor resistance towards solvent due to the lack of physical adsorption in vulcanizate. Hence, the solvent could easily penetrate the rubber chain of vulcanizate. Once APKS was added into the XNBR vulcanizate, the swelling index started to decrease where loading ratio of 5, 10, 20, 30, 40, and 50 phr of APKS obtained a swelling index value of 145.45%, 137.77%, 134.93%, 127.97%, and 117.21%, respectively. In general, it could be said that the swelling index was inversely proportional to the *Vr*. Unfilled XNBR vulcanizate showed the lowest value of *Vr* which is 0.92. As the loading ratio of APKS increased, the *Vr* of APKS-filled XNBR vulcanizates increased too. The addition of 5, 10, 20, 30, 40, and 50 phr of APKS in XNBR vulcanizate resulted in high *Vr* values which were 1.28, 2.94, 2.95, 3.43, and 4.12, respectively. The increasing *Vr* values indicated good adsorption of XNBR on the APKS surface which could be due to mechanical interlocking that occurred between the rubber and filler. Improved rubber-filler interaction between XNBR and APKS promoted the compactness of crosslinking and immobilizing the rubber chain which contributed to the improvement of swelling properties. This helped to restrict the penetration of solvent into the rubber chains which led to a decrease in swelling index [24]. As mentioned in the SEM analysis of APKS which was shown in Figure 3, the rough surface and porous structure of APKS supplied a wide surface area for sulphur to form crosslink during the process of vulcanization which resulted in the enhancement of rubber-filler interaction [25].

Bound Rubber Content (BRC) describes the interaction between rubber matrix and filler [26]. The BRC analysis determines the rubber that remains attached to the filler network when the vulcanized was extracted with solvent. The BRC results are displayed in Figure 6. Based on the results, unfilled XNBR vulcanizate showed 0% of BRC as there was no presence of APKS. With the incorporation of a high loading ratio of APKS, the BRC percentage of APKS-filled XNBR vulcanizates increased steadily for APKS loading of 5

phr to 40 phr and had a reduction in BRC percentage when 50 phr of APKS was used. This would mean that 40 phr of APKS was the optimum loading ratio for XNBR vulcanizate to obtain a high BRC percentage. The high BRC percentage would be an indication of good rubber-filler interaction. The porosity of APKS as shown in the SEM images (refer Figure 3) and the surface area of APKS which was about 491.7 m^2/g as reported in the BET analysis (refer Table 2) promoted higher rubber-filler interaction. Moreover, the irregular shape of APKS as displayed in Figure 3 enhanced the interfacial adhesion of rubber on the filler surface. The highly entangled network structure could have also trapped the molecular rubber chain into the pores of the APKS, strengthening the rubber-filler interaction. The finer particle size of the APKS which was between the ranges of 28.0 to 41.6 µm provided a large surface area for the XNBR to bind to the APKS surface. Hence, the physical interaction of rubber and filler through mechanical interlocking contributed to the increment of BRC [27].

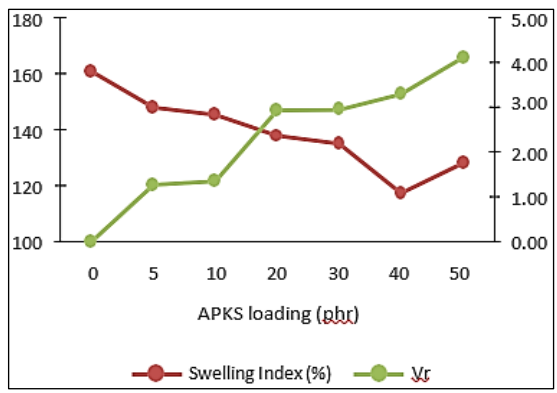

Figure 5: Swelling index measurement and volume fraction of rubber in the swollen gel, *Vr* of APKS-filled XNBR

The addition of filler provides reinforcement to rubber vulcanizates which would contribute to low volume loss (*VL*) of the rubber vulcanizate when subjected to high abrasive force. Figure 7 shows the results of the *VL* of APKS-filled XNBR vulcanizates where it could be seen that the *VL* of APKS-filled XNBR vulcanizates had a decreasing trend as the loading ratio of APKS increased. This would indicate that with higher loading of APKS, the XNBR vulcanizate exhibited higher abrasion resistance, hence it would be able to resist surface damages. The highest *VL* was observed for unfilled XNBR vulcanizate due to lack of APKS incorporation causing the XNBR vulcanizate to have low mechanical resistance towards abrasive force. The addition of 5 phr of APKS in XNBR vulcanizate reduced the *VL* by 8.9% compared to the

unfilled XNBR. As the loading ratio of APKS increased, the *VL* reduced drastically by 41.57%, 41.71%, 46.50%, 52.90%, and 58.97% for XNBR vulcanizates with APKS loading of 10 phr, 20 phr, 30 phr, 40 phr and 50 phr, respectively. This shows that APKS was able to prevent XNBR vulcanizates from having a high *VL*. The enhancement of abrasion resistance which was indicated by *VL* reduction could be attributed to the physical structure of APKS. The pores and irregular shape of APKS enhanced the physical adsorption of the rubber chain on the filler surface through mechanical interlocking, hence improving the abrasion resistance of the vulcanizate [24]. The high carbon content of APKS as shown in the EDX analysis (refer Figure 4) may have formed a covalent bond with the XNBR chain which enhanced the interaction between APKS and XNBR [7].

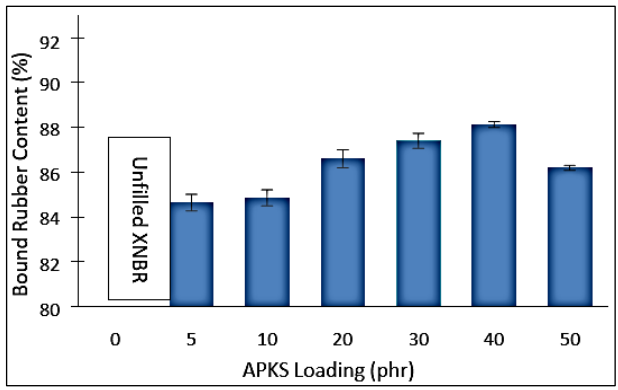

Figure 6: Bound rubber content of APKS-filled XNBR vulcanizates

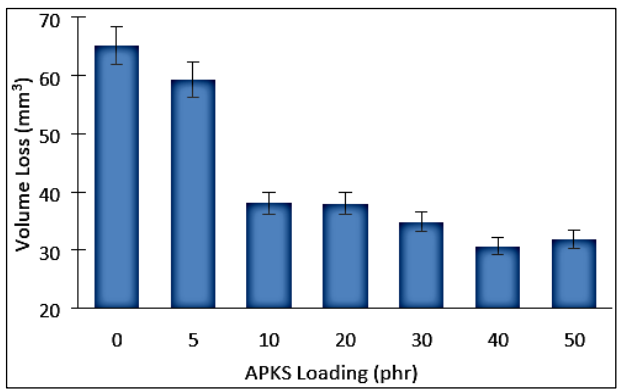

Figure 7: VL of APKS-filled XNBR vulcanizates

Compression set is an important property for a rubber vulcanizate as it measures the ability of the vulcanizate to return to the initial thickness after being subjected to a compressive force. As for hardness, it is the ability of the rubber vulcanizate to resist indentation permanently. The results of the compression set and hardness of APKS-filled XNBR vulcanizates are shown in Figure 8. Based on the results, the compression set value of the XNBR vulcanizates increased as the loading of APKS increased. A higher compression set value would mean that the XNBR vulcanizate had a poor ability to resist deformation after being compressed [26]. With this, a permanent deformation could occur and the vulcanizate would not be able to recover to its initial thickness, shape, and form. This could be due to the reduction in the rubber chain mobility as higher crosslink density was observed for XNBR vulcanizates with high loading of APKS. As the APKS loading increased, the increased crosslink density through the formation of chain segments between rubber and filler restricted the rubber chain's mobility. The rubber chain immobilization due to rubber attachment on the filler surface inhibited the elastic behaviour of rubber which eventually increased the compression set and enhanced the rigidity of vulcanizate [28]. The incorporation of 5 and 10 phr of APKS in XNBR resulted in a slight increment in compression set value of about 11.69% and 12.13%, respectively. However, by adding a higher APKS loading of 20 phr, 30 phr, 40 phr, and 50 phr, the compression set increased significantly by 17.93%, 19.81%, 20.53%, and 20.93%, respectively. The increase in the rigidity of vulcanizate corresponded to the hardness results obtained for the vulcanizate [29]. Unfilled rubber showed the lowest hardness value in comparison with the rest of APKS-filled vulcanizates whereas XNBR vulcanizate without APKS recorded a hardness value of 43 Shore A. Although the XNBR vulcanizate was without any addition of APKS, it displayed a considerably high hardness due to the XNBR's nature itself of having high hardness. However, with the incorporation of APKS, the hardness of XNBR vulcanizates was well improved and enhanced. The hardness value showed an increasing trend because the small particle size and pores of the APKS promoted crosslink density which then resulted in stiffness and rigidity of the XNBR vulcanizates. In comparison with the unfilled XNBR vulcanizate, the hardness of APKS-filled XNBR vulcanizates increased by 9.37 %, 16.40 %, 20.61 %, 25.76 %, 31.15 %, and 44.50 % with the incorporation of 5 phr, 10 phr, 20 phr, 30 phr, 40 phr and 50 phr of APKS, respectively. The enhancement of hardness was due to the improved rubber-filler interaction that was supported by the *Vr* results obtained in Figure 5 [28]. The highest hardness value (62 Shore A) was exhibited by XNBR vulcanizate with 50 phr.

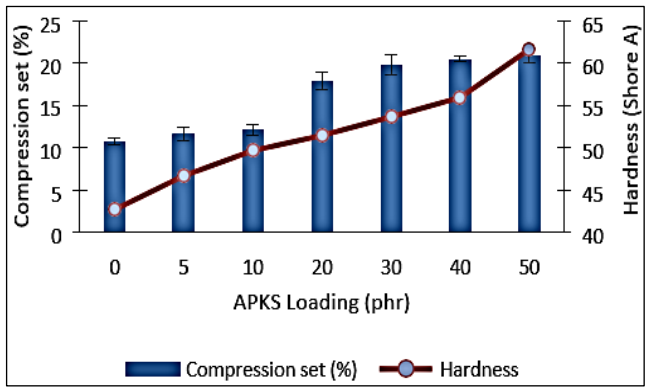

Figure 8: Compression set and hardness of APKS-filled XNBR vulcanizates

Conclusion

This study was carried out to elucidate the influence of various loading ratios of PAKS in XNBR vulcanizates. It could be concluded that APKS has the potential to be commercialized as a semi-reinforcing filler in rubber vulcanizates, specifically XNBR vulcanizates. It was observed that the incorporation of APKS in XNBR vulcanizates helped to improve the physical and mechanical properties of the XNBR vulcanizates in terms of BRC, abrasion resistance, and hardness. This was mainly due to the high surface activity of APKS which was shown in FTIR analysis, the porous structure, and irregularity in the shape of APKS. These factors helped to increase the surface area of the APKS, promoting high rubber-filler interaction and mechanical interlocking between XNBR and APKS. The average surface area, pore volume, and pore radius of the APKS sample were 491.7 m^2/g, 2.323 ± 0.197 m^3/g, and 513.9 ± 330.1 nm, respectively. Therefore, it could be said the fine particle size and wide surface area of APKS promoted the formation of crosslinking and further enhanced the rubber-filler interaction. Based on the results obtained, the optimum loading ratio of APKS in XNBR vulcanizate was 40 phr as the XNBR vulcanizate filled with 40 phr of APKS exhibited the most enhanced physical and mechanical properties such as low swelling index measurement and increased volume fraction of rubber in the swollen gel (*Vr*), BRC, abrasion resistance, and hardness. Therefore, it is proven that APKS could be used as a semi-reinforcing filler in rubber reinforcement. This would be an advantage to the rubber industry and palm oil industry as with the proof of the efficiency and effectiveness of APKS as a biofiller, rubber manufacturers would have an option for a more sustainable, eco-friendly filler and alarming issues such as the abundance of palm oil waste could be reduced

significantly. This study would encourage rubber manufacturers and researchers to incorporate APKS in their own production and studies as well, especially for specific applications such as rubber car mats and even shoe soles.

Contribution of Authors

The authors contributed equally to each part of this work. All authors reviewed and approved the final version of this work.

Funding

The APC was funded by Research Management Centre, Universiti Teknologi MARA, UiTM, under Pembiayaan Yuran Penerbitan Artikel Berindeks (PYPA).

Conflict of Interests

All authors declared that they have no conflicts of interest.

Acknowledgement

The authors would like to give thanks to the staff at the Research Institute of Malaysian Palm Oil Board (MPOB), Airelastic Industries Sdn. Bhd., Institute of Science (IOS) and Faculty of Applied Sciences of Universiti Teknologi MARA (UiTM) Shah Alam for helping with the materials' supply, and preparation of samples and tests.

References

[1] M. T. N. A. Ar-Raudhoh, M. F. M. Haziq, Z. A. Zafirah, M. S. N. Liyana and Z. N.Hayawin, "Comparative studies on cure characteristics and mechanical properties of oil palm biomass filled natural rubber composites," *Journal of Oil Palm Research,* pp. 1-12, 2023. http://doi.org/10.21894/jopr.2023.0009

[2] S. Kadandale, R. Martenb, and R. Smith, "The palm oil industry and noncommunicable diseases", *Bull World Health Organ*, vol. 97, no. 2, pp. 118-128, 2019. http://doi.org/10.2471/BLT.18.220434

[3] Z. Z. Abidin, M. Siti Nur Liyana, A. Z. Romli, S. S. Sarkawi and N. H. Zainal, "Synergistic effect of partial replacement of carbon black by palm kernel shell biochar in carboxylated nitrile butadiene rubber composites", *Polymers*, vol 15, no. 943, pp.1-13, 2023. http://doi.org/10.3390/polym15040943

[4] A. Promraksa, A. and N. Rakmak, "Biochar production from palm oil mill residues and application of the biochar to adsorb carbon dioxide", *Helicon*, vol 6, no. 5, pp. 1-9, 2020. http://doi.org/10.1016/j.helivon.2020.e04019

[5] B. Xue, J. Sui, D. Xu, Y. Zhu and X. Liu, "A facile ball milling method to produce sustainable pyrolytic rice husk biofiller for reinforcement of rubber mechanical property", *Industrial Crops and Products*, vol. 141, no. pp. 1-8, 2019. https://doi.org/10.1016/j.indcrop.2019.111791

[6] Z. Z. Abidin, M. Siti Nur Liyana, S. S. Sarkawi and S. S. Nurshamimi, "Influence of filler system on the cure characteristics and mechanical properties of butyl reclaimed rubber", *BioResources*, vol. 15, no. 3, pp. 6045-6060, 2020. https://doi.org/10.15376/biores.15.3.6045-6060

[7] Daud, S., H. Ismail, and A.A. Bakar, "A study on the curing characteristics, tensile, fatigue and morphological properties of alkali treated palm kernel shell-filled natural rubber composites", *BioResources*, vol. 12, no. 1, pp. 1-15, 2017. http://dx.doi.org/10.15376/biores.12.1.1273-1287

[8] N. A. M. Aini, N. Othman, M. H. Hussin, K. Sahakaro and N. Hayeemasae, "Lignin as alternative reinforcing filler in the rubber industry: A review", *Frontiers in Materials*, vol. 6, pp. 1-18, 2020. https://doi.org/10.3389/fmats.2019.00329

[9] M. Siti Nur Liyana, S. Nur Atiqah, H. Rossuraiti Dol, A. T. Amirah Amalina and S. S. Sarkawi, "Influence of Si-69 treated hybrid carbon black/precipitated calcium carbonate filler on the crosslink density and physico-mechanical properties of nr/sbr blends," *ARPN Journal of Engineering and Applied Sciences*, vol. 14, no. 20, pp. 7771-7777, 2019. http://dx.doi.org/10.36478/jeasci.2019.7771.7777

[10] S. H. Kong, H. Zainal, S. K. Loh and S-H. Kong, "Palm kernel shell biochar production, characterization and carbon sequestration potential," *Journal of Palm Oil Research*, vol. 31, no. 3, pp. 508-520, 2019. http://doi.org/10.21894/jopr.2019.0041

[11] P. Wang, J. Zhang, Q. Shao, "Physicochemical properties evolution of chars from palm kernel shell pyrolysis," *Journal of Thermal Analysis and Calorimetry*, vol. 133, no. 3, pp. 1271-1280, 2018. https://doi.org/10.1007/s10973-018-7185-z

[12] S. E. Rahim, S. B. Wan Yussof, H. Olalere, O. A, and O. A. Habeeb, "Morphological, thermal stability and textural elucidation of raw and activated palm kernel shell and their potential use as environmental-

friendly adsorbent", *Chemical Data Collections*, vol. 21, pp. 1-8, 2019. https://goi.org/10.1016/j.cdc.2019.100235

[13] S. Amin, R. T. Bachmann, and S.K. Yong, "Oxidised biochar from palm kernel shell for eco-friendly pollution management", *Scientific Research Journal*, vol. 17, no. 2, pp. 44-66, 2020. https://doi.org/10.24191/srj.v17i2.10001

[14] S. Greenough, M. J. Dumont, and S. Prasher, "The physicochemical properties of biochar and its applicability as a filler in rubber composites: A review", *Materials Today Communications*, vol. 29, p. 102912, 2021. https://doi.org/10.1016/j.mtcomm.2021.102912

[15] M. Siti Nur Liyana, B. Fauzi, S. N. F. Roslan and R. Fauzi, "Hybridized reinforcement of natural rubber/styrene butadiene rubber (NR/SBR) blend with treated bis (3-Triethoxysilylpropryl) tetrasulfide (Si-69)-hybrid carbon black/nanocalcium carbonate filler: Mooney viscosity, crosslink density and cure characteristic," *ARPN Journal of Engineering and Applied Sciences*, vol. 14, no. 17, pp. 6208-6212, 2019.

[16] A. Omri, M. Benzina, "Removal of manganese (II) ions from aqueous solutions by adsorption on activated carbon derived a new precursor: Ziziphus spina-christi seeds," *Alexandria Engineering Journal,* vol. 51, no. 4, pp. 343-350, 2012. https://doi.org/10.1016/j.aej.2012.06.003

[17] A.K Sakhiya, A. Anand, and P. Kaushal, "Production, activation, and application of biochar in recent times", *Biochar*, vol. 2, pp. 253-285, 2020. https://doi.org/10.1007/s42773-020-00047-1

[18] S.N.L. Mamauod, F. Basirah, S. Nor Atiqah, F. Roslinda and A. Z. Romli, "Preparation and Characterization of Treated Bis [3-(Triethoxysilyl) Propoyl] Tetrasulfide (Si-69)-Hybrid CB/PCC Fillers Reinforced NR/SBR Composites: Cure characteristics, mooney viscosity and crosslink density", *Advanced Composites Letters*, vol. 27, no. 6, pp. 261-265, 2018. https://doi.org/10.1177/096369351802700602

[19] B. C. Fernandes, K. F. Mendes, A. F. Dias Junior, V. P. da Silva, T.M. da Silca Teofilo, T.S. Valadao, "Impact of pyrolysis temperature on the properties of eucalyptus wood-derived biochar", *Materials*, vol. 13, no. 24, pp. 1-13, 2020. https://doi.org/10.3390%2Fma13245841

[20] G. Chang, X. Han, P. Qi, M. An, X. Hu, and Q. Guo, "Characteristics of reactivity and structures of palm kernel shell (pks) biochar during co_2/h_2o mixture gasification," *Chinese Journal of Chemical Engineering*, vol. 26, no. 10, pp. 2153-2161, 2018. https://doi.org/10.1016/j.cjche.2018.03.003

[21] K. Y. Cheong, Z. Haryati, L. Soh Kheang, and K. Sieng-Huat, "Palm kernel shell biochar production, characteristics and carbon sequestration potential," *Journal of Oil Palm Research,* vol. 31, no. 3, pp. 508-520, 2019. http://doi.org/ 10.21894/jopr.2019.0041

[22] W. R. Aziz, S. M. A. Hamdan, S. and Z. Ngaini, "Biochar production from agricultural wastes via low-temperature microwave carbonization,"

2015 IEEE International RF and Microwave Conference (RFM), pp. 244-247, 2015. http://doi:10.1109/rfm.2015.7587754

[23] R. K. Liew, M.Y. Chong, O.U. Osazuwa, W.L. Nam, X. Y. Phang, M. H. Su, C. K. Cheng, C. K., C.T. Chong, and S. S. Lam, "Production of activated carbon as catalyst support by microwave pyrolysis of Palm Kernel Shell: A comparative study of chemical versus physical activation", *Research on Chemical Intermediates*, vol. 44, no. 6, pp. 3849-3865, 2018. https://doi.org/10.1007/s11164-018-3388-y

[24] D. Y. Kim, J. W. Park, D. Y. Lee and K. H. Seo, "Correlation between the Crosslink Characteristics and Mechanical Properties of Natural Rubber Compound via Accelerators and Reinforcement", *Polymers*, vol. 12, no. 9, pp. 1-14, 2020. https://doi.org/10.3390/polym12092020

[25] D. M. Paleri, A. Rodriguez-Uribe, M. Misra and A. K. Mohanty, "Preparation and characterization of eco-friendly hybrid biocomposites from natural rubber, biocarbon, and carbon black", *Express Polymer Letters*, vol, 15, no. 3, pp. 236–249, 2021. https://doi.org/10.3144/expresspolymlett.2021.21

[26] S. S. Sarkawi, A. K. C. Aziz, and A. N. Kamaruddin, "Properties of epoxidized natural rubber tread compound: the hybrid reinforcing effect of silica and silane system", *Polymers & Polymer Composites*, vol. 24, no. 9, no. 775-782, 2016. https://doi.org/10.1177/096739111602400914

[27] O. Somseemee, P. Sae-Oui, C. Siriwong, "Reinforcement of surface-modified cellulose nanofibrils extracted from napier grass stem in natural rubber composites", *Industrial Crops and Products*, vol. 171, pp. 1-11, 2021. https://doi.org/10.1016/j.indcrop.2021.113881

[28] D. M Paleri, A. Rodriguez-Uribe, M. Misra, A. K. Mohanty, "Preparation and characterization of eco-friendly hybrid biocomposites from natural rubber, biocarbon, and carbon black", *Express Polymer Letters*, vol. 15, no. 3, pp. 236–249, 2021. doi:10.3144/expresspolymlett.2021.21

[29] M. Lay, A. Rusli, M. K. Abdullah, Z. A. A. Hamid and R. K. Shuib, "Converting dead leaf biomass into activated carbon as a potential replacement for carbon black filler in rubber composites", *Composites Part B: Engineering*, vol. 201, pp. 1-10, 2020. https://doi.org/10.1016/j.compositesb.2020.108366